

ADVANCED MATERIALS

Supporting Information

for *Adv. Mater.*, DOI: 10.1002/adma.201601609

Bioinspired 1D Superparamagnetic Magnetite Arrays with
Magnetic Field Perception

*Xiangyu Jiang, Jiangan Feng, Lei Huang, Yuchen Wu, Bin
Su, Wensheng Yang,* Liqiang Mai,* and Lei Jiang*

Supporting Information

Bioinspired one-dimensional superparamagnetic magnetite arrays with magnetic field perception

Xiangyu Jiang,[†] Jiangan Feng,[†] Lei Huang, Yuchen Wu, Bin Su, Wensheng Yang*, Liqiang Mai*, Lei Jiang*

[*] Dr. X.Y. Jiang, Prof. L. Jiang, Prof. W.S. Yang
State Key Laboratory of Supermolecular Structure and Materials, College of Chemistry,
Jilin University, Changchun 130012, P. R. China
jjanglei@iccas.ac.cn
wsyang@jlu.edu.cn

Dr. J.G. Feng, Dr. Y.C. Wu, Prof. L. Jiang
Laboratory of Bioinspired Smart Interfacial Science, Technical Institute of Physics and
Chemistry, Chinese Academy of Sciences, Beijing 100190, P. R. China

Mr. L. Huang, Prof. L.Q. Mai
State Key Laboratory of Advanced Technology for Materials Synthesis and Processing,
Wuhan University of Technology, Wuhan 430070, China
mlq518@whut.edu.cn.

Dr. B. Su
Department of Chemical Engineering, Monash University, Clayton, Victoria 3800,
Australia.

[†] These authors contributed equally to this work.

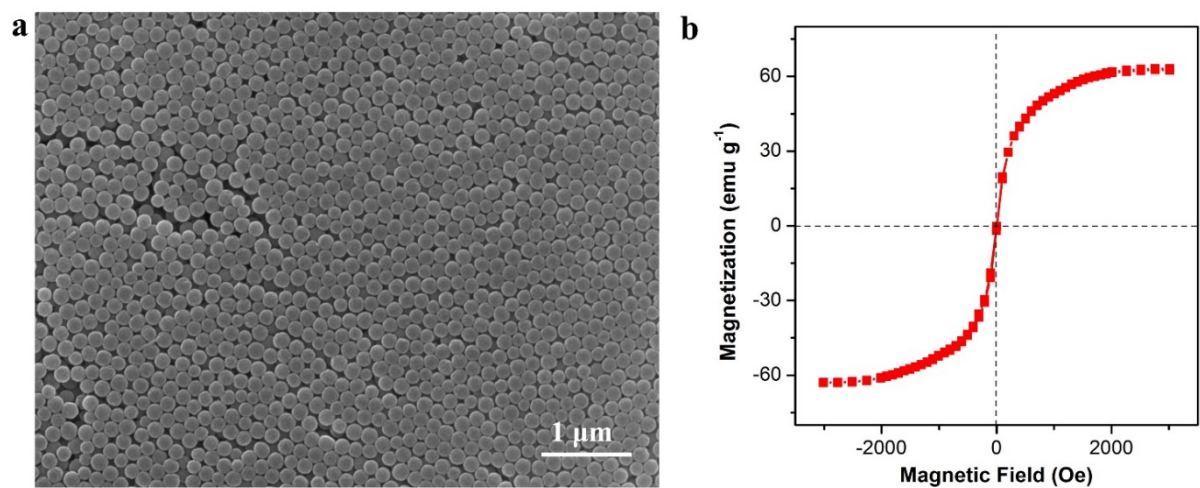


Figure S1. SEM image and magnetization curve of Fe₃O₄ nanoparticles. a) SEM image showing Fe₃O₄ nanoparticles with uniform size of ~150 nm. b) Magnetization curve of Fe₃O₄ nanoparticles indicating the superparamagnetic nature with saturated magnetization of 62.3 emu g⁻¹.

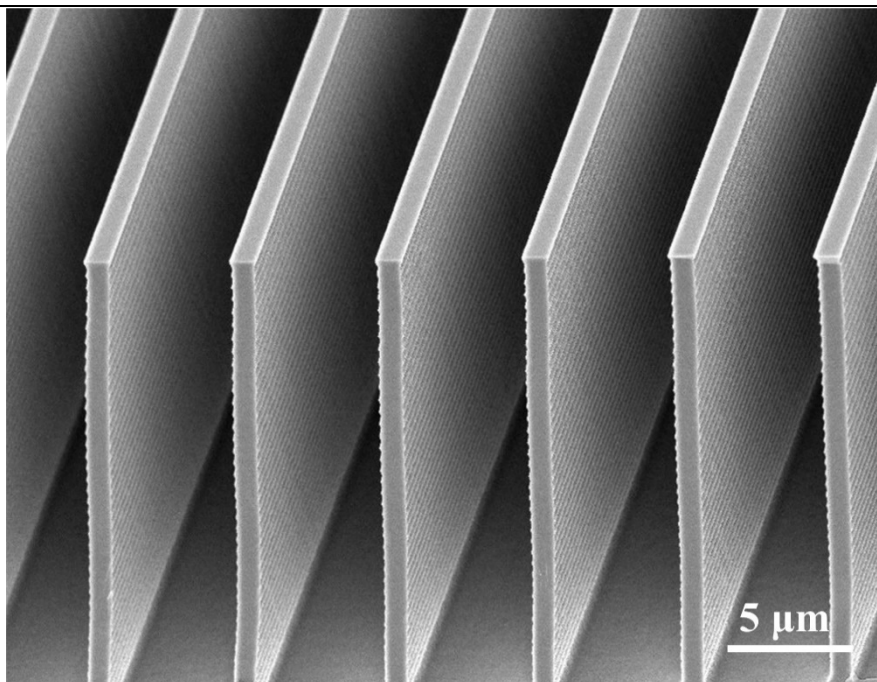


Figure S2. SEM image of micropillar-structured template with width of 2 μm , gap of 5 μm and height of 20 μm .

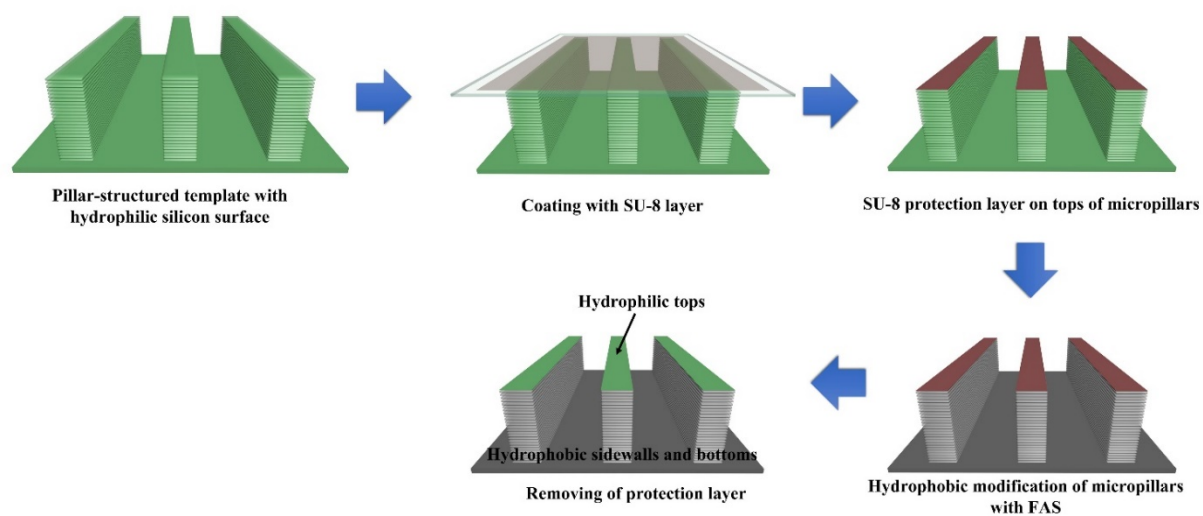


Figure S3. Schematic illustration of selected modification process of top-hydrophilic, sidewall&bottom-hydrophobic micropillar-structured template. A SU-8 layer was employed as protection layer on tops followed by hydrophobic modification using FAS, which formed hydrophilic tops, hydrophobic sidewalls and bottoms after removing protection layer.

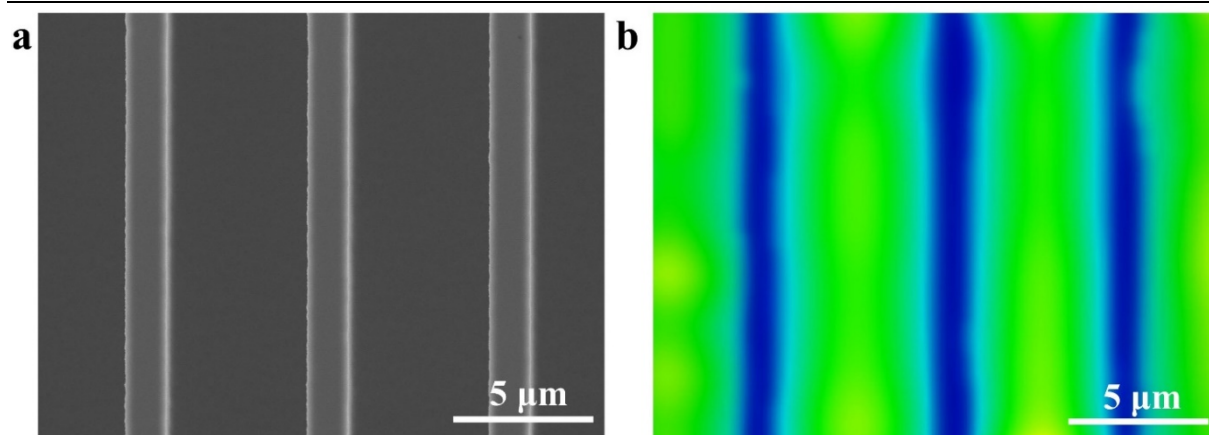


Figure S4. Spatial distribution of FAS on micropillar-structured template after selected modification. a) SEM image of micropillar-structured template after modification. b) Raman mapping showing high-intensity Raman signal at bottom and gap regions, whereas nearly no FAS signals can be detected at the top regions.

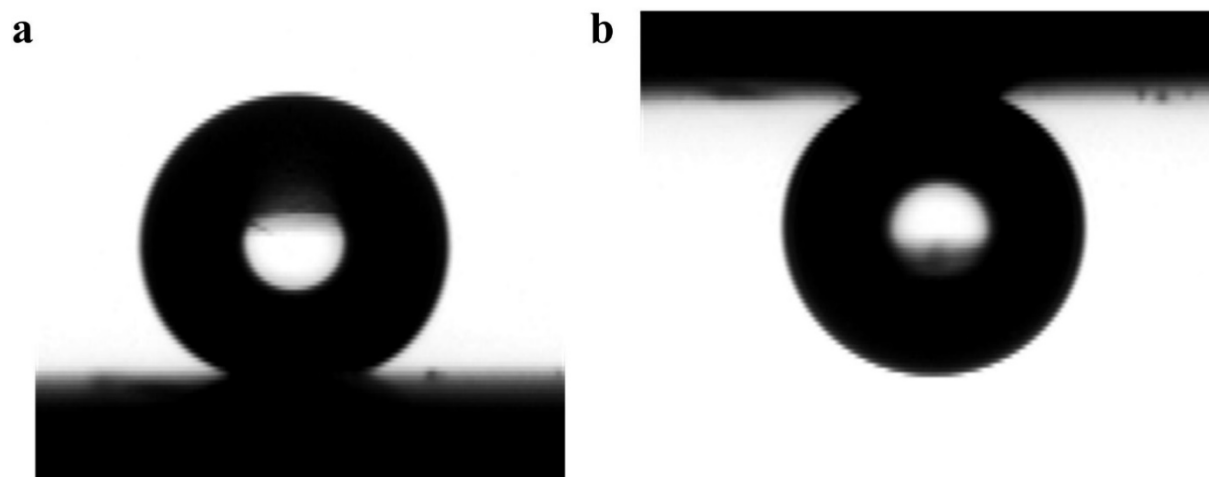


Figure S5. Water contact angle (CA) measurement of micropillar-structured template after FAS modification. a) High CA of $155.2 \pm 2.3^\circ$ indicates the superhydrophobicity induced by the low-surface-energy modification of sidewalls and gaps, which traps air cushions to lift the water drops. b) CA measurement on an inverted micropillar-structured substrate. Owing to the hydrophilicity of the micropillars' tops, the water drop can be anchored onto the micropillars.

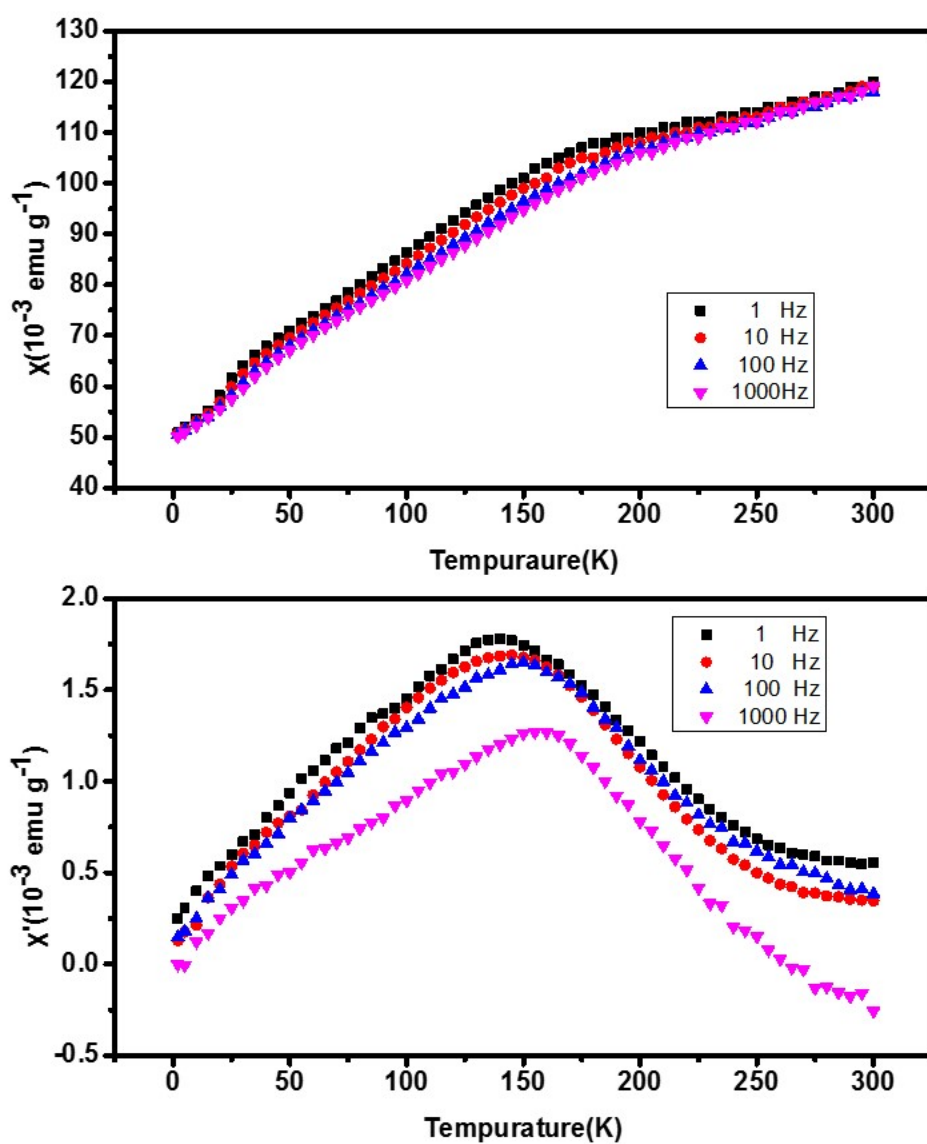


Figure S6. AC susceptibility under different frequencies between 2-300 K, Sample dosage of 10 mg. The frequencies are 1 Hz, 10 Hz, 100 Hz and 1000Hz.